Unbound-to-bound transition of two-atom polaritons in an optical cavity

Qing Sun, Jie Hu, Lin Wen, Han Pu, and An-Chun Ji

Phys. Rev. A **98**, 033801 — Published 4 September 2018

DOI: 10.1103/PhysRevA.98.033801

Unbound to bound transition of two-atom polaritons in an optical cavity

Qing Sun,[1] Jie Hu,[1] Lin Wen,[2] Han Pu,[3,*] and An-Chun Ji[1,†]

[1]*Department of Physics, Capital Normal University, Beijing 100048, China*
[2]*College of Physics and Electronic Engineering, Chongqing Normal University, Chongqing, 401331, China*
[3]*Department of Physics and Astronomy and Rice Quantum Institute, Rice University, Houston, Texas 77251, USA*

(Dated: August 10, 2018)

We consider two spin-1/2 fermions inside an optical cavity which supports a single-mode quantized light field. We demonstrate that, the atom-light coupling (ALC) gives rise to the two-atom polariton states, where the two atoms are highly entangled with cavity photons. We focus on the case where the cavity light is on resonant with the bare atomic transition. We show that, in the absence of inter-atomic interaction, the polariton is unbound, has finite center-of-mass momentum, and contains no atomic spin singlet fraction in its ground state. When strong attractive inter-atomic contact interaction is present, a stable bound polariton state exists when the ALC strength is below a critical value. When the ALC strength exceeds the critical value, a first-order transition is observed and the bound polariton becomes unbound. The first-order transition is characterized by abrupt changes of various quantities associated with the polariton and should be readily detectable.

PACS numbers:

With the successful realization of cold atoms loaded into optical cavities [1, 2], cavity quantum electrodynamics (QED) with ultracold atoms [3–5] has attracted enormous attentions and provided a unique platform to explore exotic collective quantum behaviors of the hybrid atom-cavity systems [6–28]. For example, the noted Dicke superradiance transition [29, 30] has been realized in cavity-Bose-Einstein-condensate (BEC) systems [9, 10] and then extended to Fermi gases [12–14]. These researches reveal the important effects brought by the external center-of-mass (COM) motion of atoms in the dispersive coupling regime [5]. On the other hand, the inter-atomic interactions may also compete with the atom-light coupling (ALC) dramatically, resulting in the superradiant solid in cavity-Rydberg system [16].

Another recent breakthrough is the realization of synthetic non-Abelian gauge potentials, that provide a coupling between the atomic COM motion and its internal degrees of freedom by implementing two Raman beams on ultracold atoms, forming an effective spin-orbit coupling (SOC) [31–36]. This SOC has stimulated numerous studies and underlies a variety of novel manybody phenomena [37–42]. In recent proposals [43–47], one of the Raman beams is replaced by an optical cavity field. It was shown that, cavity-assisted two-photon Raman transition can give rise to dynamical SOC with many intriguing nonlinear properties.

In this paper, we investigate the two-atom ground state properties of an attractive two-component Fermi gas inside an optical cavity. In contrast to the classical Raman beams, the cavity field is quantized and causes the nonlocal atom-light coupling (ALC). The cavity photons entangle with the atoms and interplay with the inter-atomic interactions, which results in an exotic two-atom polariton state. Tuning of the ALC strength can induce a first-order phase transition in this exotic polariton, which changes between a bound and an unbound state. Accompanying with this transition, the entanglement entropy, the photon population, and the atomic spin singlet fraction associated with the polariton state exhibit discontinuous jumps across the critical ALC strength. With progress in experimental techniques of atom-cavity system, our study has interesting implications for future experiments.

The Model. – We consider a two-component Fermi gas coupled to a single-mode cavity field with wave vector $\mathbf{k}_c$ and frequency ω_c, which can be implemented by a unidirectional optical ring cavity [44, 48–50]. Under rotating wave approximation, the Hamiltonian of the system is given by $\hat{H} = \hbar\omega_c\hat{a}^\dagger\hat{a} + \hat{H}_{\rm atom} + \hat{H}_{\rm a|c}$. Here $\hat{a}$ denotes the annihilation operator of the single-mode light field. $\hat{H}_{\rm atom} = \sum_{\sigma=\uparrow,\downarrow}\int d^3\mathbf{r}[\hat{\psi}^\dagger_\sigma(\mathbf{r})(\frac{\hat{\mathbf{P}}^2}{2m} + \epsilon_\sigma)\hat{\psi}_\sigma(\mathbf{r})] + \hat{H}_{\rm int}$ describes the atoms moving inside the cavity, where $\hat{\psi}_\sigma(\mathbf{r})$ denotes the annihilation operators of the atomic state σ $(=\uparrow,\downarrow)$ at position $\mathbf{r}$, $\epsilon_{\uparrow,\downarrow} = \pm\frac{\hbar\omega_a}{2}$ represents the bare atomic energies, and $\hat{H}_{\rm int} = U\int d\mathbf{r}\hat{n}_\uparrow(\mathbf{r})\hat{n}_\downarrow(\mathbf{r})$ describes the atomic interaction with $\hat{n}_\sigma(\mathbf{r}) = \hat{\psi}^\dagger_\sigma(\mathbf{r})\hat{\psi}_\sigma(\mathbf{r})$. The ALC is described by $\hat{H}_{\rm a|c} = \int d\mathbf{r}g(\mathbf{r})[\hat{\psi}^\dagger_\uparrow(\mathbf{r})\hat{\psi}_\downarrow(\mathbf{r})\hat{a} + {\rm h.c.}]$, with the coupling strength $g(\mathbf{r}) = g_0e^{i\mathbf{k}_c\cdot\mathbf{r}}$ and g_0 the single photon Rabi frequency. Through a gauge transformation

$$\hat{\psi}_{\uparrow,\downarrow} \longrightarrow e^{\mp i\mathbf{k}_c\cdot\mathbf{r}/2}\hat{\psi}_{\uparrow,\downarrow}\,,$$

we can eliminate the position-dependent phase factor in $g(\mathbf{r})$ [51], and the total Hamiltonian in momentum space

*Electronic address: hpu@rice.edu
†Electronic address: anchun.ji@cnu.edu.cn

can be written as $\hat{H} = \hat{H}_0 + \hat{H}_{\rm int}$, where

$$\hat{H}_0 = \hbar\omega_c \hat{a}^\dagger \hat{a} + \sum_{\mathbf{k},\sigma} \varepsilon_{\mathbf{k}\sigma} \hat{\psi}^\dagger_{\mathbf{k}\sigma} \hat{\psi}_{\mathbf{k}\sigma} + \sum_{\mathbf{k}} g_0 (\hat{\psi}^\dagger_{\mathbf{k}\uparrow} \hat{\psi}_{\mathbf{k}\downarrow} \hat{a} + h.c.),$$

$$\hat{H}_{\rm int} = \frac{U}{V} \sum_{\mathbf{k},\mathbf{k}',\mathbf{q}} \hat{\psi}^\dagger_{\mathbf{q}/2+\mathbf{k}\uparrow} \hat{\psi}^\dagger_{\mathbf{q}/2-\mathbf{k}\downarrow} \hat{\psi}_{\mathbf{q}/2-\mathbf{k}'\downarrow} \hat{\psi}_{\mathbf{q}/2+\mathbf{k}'\uparrow}, \quad (1)$$

where $\varepsilon_{\mathbf{k},\uparrow(\downarrow)} = \frac{\hbar^2}{2m}(\mathbf{k} \pm \lambda \mathbf{e}_z)^2 \pm \frac{1}{2}\hbar\omega_a$ with $\lambda \equiv |\mathbf{k}_c|/2$, and we define $\mathbf{k}_c$ to be along the z-axis of the cavity. Note that, the atomic part $\varepsilon_{\mathbf{k}}$ is formally equivalent to that of the one-dimensional spin-orbit coupling [31]. The contact attractive interaction U between atoms (e. g. ^{6}Li, ^{40}K, etc.) is well captured by the low-energy s-wave scattering length a_s, which should be regularized as $\frac{m}{4\pi\hbar^2 a_s} = \frac{1}{U} + \frac{1}{V}\sum_{\mathbf{k}} \frac{1}{2\epsilon_{\mathbf{k}}}$ with $\epsilon_{\mathbf{k}} = \frac{\hbar^2\mathbf{k}^2}{2m}$ and V being the quantization volume [52]. For simplicity, we take $m = \hbar = 1$.

In the case of a single atom, we can easily diagonalize $\hat{H}_0$ to find its spectrum [53]. Here the total excitation number $N_e \equiv \hat{a}^\dagger \hat{a} + \sum_{\mathbf{k}} \hat{\psi}^\dagger_{\mathbf{k},\uparrow} \hat{\psi}_{\mathbf{k},\uparrow}$ is conserved. For given $N_e = N$, the spectrum contains two branches, and the dispersion of the lower branch is given by

$$E_-(\mathbf{k}) = (N-1)\omega_c + \frac{\omega_c + \mathbf{k}^2 + \lambda^2}{2} - \sqrt{(k_z\lambda + \delta/2)^2 + N g_0^2},$$

where $\delta = \omega_a - \omega_c$ denotes the atom-cavity detuning. For $\delta = 0$, i.e., when the cavity photons are resonant with the bare atomic transition, which will be the focus of this work, there exists a critical ALC strength $g_c = \lambda^2/\sqrt{N}$. When $g_0 < g_c$, the ground state is doubly degenerate and occurs at $k_z = \pm q_{\rm min} = \pm\sqrt{\lambda^4 - N g_0^2}/\lambda$. When $g_0 \geq g_c$, $q_{\rm min} = 0$ and the two degenerate ground states merges into a single one. $q_{\rm min}$ as a function of g_0 is plotted in Fig. 1(b) as the dotted line.

It is noteworthy that, the above single-atom polariton spectrum under constant excitation number is similar to the single-atom spectrum of the SOC system induced by the classical Raman field [31]. However, when we consider two-atom problem, the atom-cavity system would differ significantly from the classical field system. As it is well known, in the absence of atomic interactions, the energy of two atoms coupled to a classical field would be simply given by the sum of the individual single-atom energies. By contrast, when the two atoms are coupled to a cavity field, the latter can induce an effective interatomic interaction. As a result, the two atoms can no longer be regarded as independent from each other. In fact, they will be entangled with the cavity photons and form a nontrivial unbound two-atom polariton continuum. We now turn to study the properties of such an unbound polariton in detail.

Unbound two-atom polariton continuum. – In the absence of the s-wave interaction, $U = 0$. The momentum of the two atoms are individually conserved. Take the momentum of the atoms to be $\mathbf{k}_1 = \frac{\mathbf{q}}{2} + \mathbf{k}$ and $\mathbf{k}_2 = \frac{\mathbf{q}}{2} - \mathbf{k}$ ($\mathbf{k}$ and $\mathbf{q}$ are the relative and the COM momenta, respectively) and a fixed excitation excitation N (we assume $N > 1$), the wave function of the unbound two-atom polariton (UP) can be written as

$$\begin{aligned}\Phi_{\mathbf{k},\mathbf{q}} &= \varphi^{\uparrow\downarrow}_{\mathbf{k},\mathbf{q}} \hat{\psi}^\dagger_{\mathbf{k}_1\uparrow} \hat{\psi}^\dagger_{\mathbf{k}_2\downarrow} |N-1\rangle + \varphi^{\downarrow\uparrow}_{\mathbf{k},\mathbf{q}} \hat{\psi}^\dagger_{\mathbf{k}_1\downarrow} \hat{\psi}^\dagger_{\mathbf{k}_2\uparrow} |N-1\rangle \\ &+ \varphi^{\uparrow\uparrow}_{\mathbf{k},\mathbf{q}} \hat{\psi}^\dagger_{\mathbf{k}_1\uparrow} \hat{\psi}^\dagger_{\mathbf{k}_2\uparrow} |N-2\rangle + \varphi^{\downarrow\downarrow}_{\mathbf{k},\mathbf{q}} \hat{\psi}^\dagger_{\mathbf{k}_1\downarrow} \hat{\psi}^\dagger_{\mathbf{k}_2\downarrow} |N\rangle, \quad (2)\end{aligned}$$

where $|n\rangle = \frac{1}{\sqrt{n!}}(\hat{a}^\dagger)^n |0\rangle$ denotes the n-photon Fock state. From the Schödinger equation $\hat{H}_0 \Phi_{\mathbf{k},\mathbf{q}} = E_{\mathbf{k},\mathbf{q}} \Phi_{\mathbf{k},\mathbf{q}}$, one can derive the equation for the eigenenergy $E_{\mathbf{k},\mathbf{q}}$, which is given by

$$E_{\mathbf{k},\mathbf{q}} = \mathcal{E}_{\mathbf{k},\mathbf{q}} + \epsilon_{\frac{\mathbf{q}}{2}+\mathbf{k}} + \epsilon_{\frac{\mathbf{q}}{2}-\mathbf{k}} + \frac{k_c^2}{4} + (N-1)\omega_c, \quad (3)$$

where

$$\mathcal{E}_{\mathbf{k},\mathbf{q}} = \frac{2(N-1)g_0^2}{\mathcal{E}_{\mathbf{k},\mathbf{q}} - \delta - k_c q_z/2} + \frac{2N g_0^2}{\mathcal{E}_{\mathbf{k},\mathbf{q}} + \delta + k_c q_z/2} + \frac{(k_c k_z)^2}{\mathcal{E}_{\mathbf{k},\mathbf{q}}}. \quad (4)$$

The first and second terms at the r.h.s. of Eq. (4) describe the energy corrections from processes of first annihilating and then creating a photon and vice versa, while the third term originates from the singlet component induced by the finite momentum transfer from photons. Due to the ALC, $E_{\mathbf{k},\mathbf{q}}$ consists of four branches forming the continuum. The ground state energy of the UP is given by the minimum of the lowest branch, which is also the threshold of the continuum spectrum, hence we denote it as $E_{\rm th}$. In Fig. 1(a), we plot $E_{\rm UP} \equiv E_{\rm th} - (N-1)\omega_c$ as a function of the ALC strength g_0, where $(N-1)\omega_c$ is the ground state energy in the limit of $g_0 = 0$ for excitation number N and $\delta = 0$. One can see that $E_{\rm UP}$ is a decreasing function of g_0, which scales as g_0 for large g_0, and as $\sqrt{N}$ for large excitation number N.

By solving the Schrödinger equation, we can also obtain the wave function. The wave function represented by Eq. (2) can be decomposed into triplet and singlet components. In particular, the singlet component is given by $\varphi_s^{\mathbf{k},\mathbf{q}} = \frac{1}{\sqrt{2}}(\varphi^{\uparrow\downarrow}_{\mathbf{k},\mathbf{q}} - \varphi^{\downarrow\uparrow}_{\mathbf{k},\mathbf{q}})$ and can be shown to be proportional to k_z, the z-component of the relative momentum between the two atoms (see the Appendix A). Numerically solving the Eq. (4) to obtain the minimal energy, we find that the ground state UP always have $k_z = 0$, hence the ground state UP is purely spin triplet.

Next, we address the question concerning the COM momentum of the ground state UP, denoted as $\mathbf{q}_{\rm UP}$. Our calculation shows that $\mathbf{q}_{\rm UP} = q_{\rm UP}\hat{\mathbf{e}}_z$ is always nonzero. In Fig. 1(b) we plot $q_{\rm UP}$ as a function of g_0. In the limit of small g_0, we have

$$q_{\rm UP} \simeq k_c \sqrt{1 - (4N-2)(g_0/E_c)^2}\,.$$

When $g_0 = 0$, $q_{\rm UP} = k_c$ which is twice the ground state momentum of a single atom $q_{\rm min}$. However, for finite g_0, we have $q_{\rm UP} \neq 2q_{\rm min}$. In particular, when $g_0 \geq g_c = \lambda^2/\sqrt{N}$, $q_{\rm min}$ vanishes, whereas $q_{\rm UP}$ remains finite and approaches $k_c/(4N-2)$ in the limit of large g_0. This is in qualitative difference when the SOC is induced by

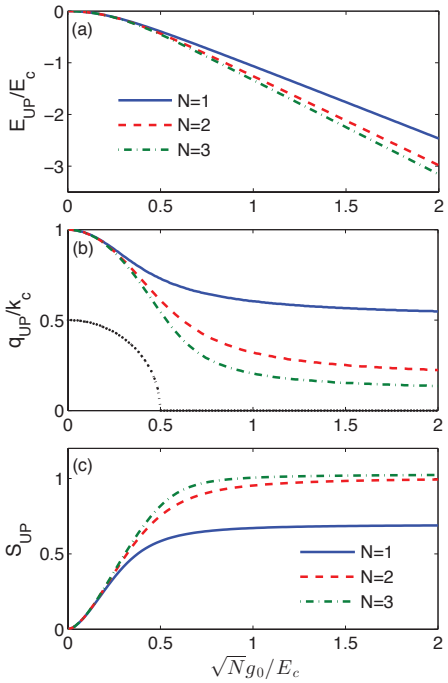

FIG. 1: (Color online) (a) Energy $E_{\rm UP}$, (b) COM momentum $q_{\rm UP}$, and (c) atom-photon entanglement entropy of the ground state of unbound two-atom polariton (UP) as functions of the normalized ALC strength $\sqrt{N}g_0/E_c$ ($E_c \equiv k_c^2/2$) for $\delta = 0$, with excitation number $N = 1$ (blue solid line), $N = 2$ (red dashed line), and $N = 3$ (greed dash-dotted line), respectively. For comparison, the momentum of the ground state of the single-atom polariton is also plotted in (b) as black dotted line.

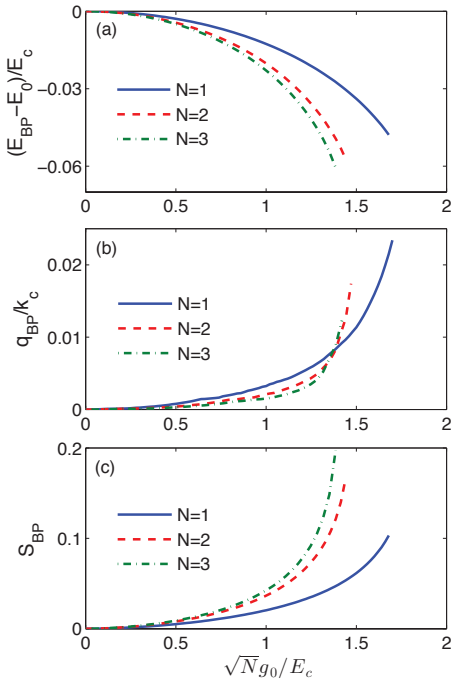

FIG. 2: (Color online) (a) Energy $E_{\rm BP} - E_0$, where E_0 is the energy of the system in the limit $g_0 = 0$, (b) COM momentum $q_{\rm BP}$, and (c) atom-photon entanglement entropy of the bound two-atom polariton (BP) as functions of the normalized ALC strength $\sqrt{N}g_0/E_c$ for $\delta = 0$ and $(k_c a_s)^{-1} = 1$, with excitation number $N = 1$ (blue solid line), $N = 2$ (red dashed line), and $N = 3$ (greed dotted line).

classical laser beams, in which case, the COM momentum of a two-atom system should just be $2q_{\rm min}$ regardless of the atom-photon coupling strength, and hence vanishes in the limit of large g_0. In our system, this classical limit is reached when the excitation number N becomes large. For small N, however, photon number fluctuation is significant and the quantum result deviates away from the classical limit.

Finally, we consider the entanglement between the atoms and the cavity field, which can be quantified by the von Neumann entanglement entropy defined as $S \equiv -{\rm tr}\rho_A \ln \rho_A$, where ρ_A is the reduced density matrix for either atoms or photons (see the Appendix C). Figure 1(c) depicts the entanglement entropy $S_{\rm UP}$ for the ground state UP as a function of g_0. $S_{\rm UP}$ increases as g_0 and saturates at a value of $\ln 2 + \ln(2N-1)/2 - N\ln N/(4N-2) - (N-1)\ln(N-1)/(4N-2)$ in the limit of large g_0.

Bound two-atom polaritons. – Now we turn to consider the attractive atomic interactions, which favors the singlet pairing between the two atoms. We are interested in the regime with $a_s > 0$ [54] and hence the two atoms, together with cavity photons, can form a bound polariton (BP). First we note that, the s-wave interaction term $\hat{H}_{\rm int}$ in Eq. (1) has no effect on the triplet component of the UP wave function. As a result, the ground state UP remains as an eigenstate of the full Hamiltonian $\hat{H}$. In general, however, the inter-atomic interactions can mix states with different relative momentum $\mathbf{k}$, and only conserve the COM momentum $\mathbf{q}$. Therefore, a general wave function of BP with COM momentum $\mathbf{q}$ for a given excitation number N can be written as

$$\Psi_{\mathbf{q}} = \sum\nolimits_{\mathbf{k}}{}' \Phi_{\mathbf{k},\mathbf{q}}\,, \tag{5}$$

where the summation over the relative momentum $\sum'_{\mathbf{k}}$ is limited to $k_z \geq 0$, and $\Phi_{\mathbf{k},\mathbf{q}}$ takes the same form as the UP wave function given in Eq. (2). Putting this into the Schrödinger equation $\hat{H}\Psi_{\mathbf{q}} = E_{\mathbf{q}}\Psi_{\mathbf{q}}$, we can find that the eigenenergy $E_{\mathbf{q}}$ is given by

$$E_{\mathbf{q}} = \mathcal{E}'_{\mathbf{k},\mathbf{q}} + \epsilon_{\frac{\mathbf{q}}{2}+\mathbf{k}} + \epsilon_{\frac{\mathbf{q}}{2}-\mathbf{k}} + \frac{k_c^2}{4} + (N-1)\omega_c, \tag{6}$$

where $\mathcal{E}'_{\mathbf{k},\mathbf{q}}$ satisfies (see the Appendix B)

$$\sum_{\mathbf{k}}\left[\left(\mathcal{E}'_{\mathbf{k},\mathbf{q}} - \frac{k_c^2 k_z^2}{\mathcal{E}'_{\mathbf{k},\mathbf{q}} - \frac{2Ng_0^2}{\mathcal{E}'_{\mathbf{k},\mathbf{q}}+\delta+k_c q_z/2} - \frac{2(N-1)g_0^2}{\mathcal{E}'_{\mathbf{k},\mathbf{q}}-\delta-k_c q_z/2}}\right)^{-1} + \frac{1}{2\epsilon_{\mathbf{k}}}\right] = \frac{V}{4\pi a_s}. \tag{7}$$

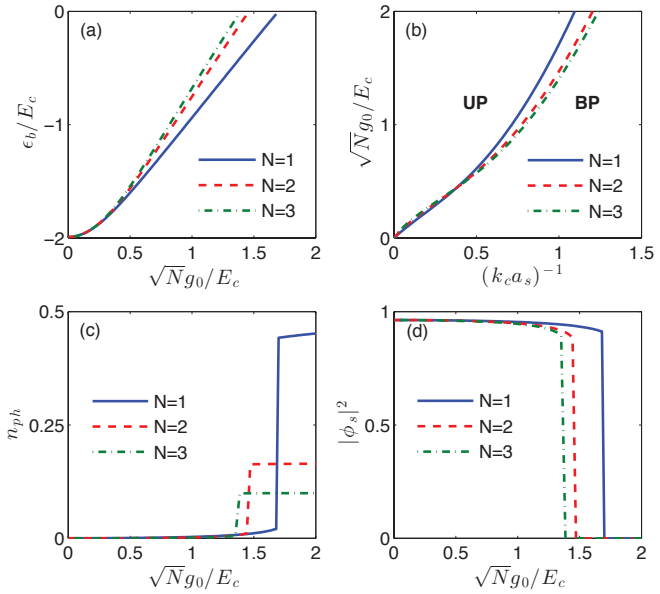

FIG. 3: (Color online) (a) ϵ_b (the energy of the BP with respect to the continuum threshold) as a function of the normalized ALC strength $\sqrt{N}g_0/E_c$ for $\delta = 0$ and $(k_c a_s)^{-1} = 1$. (b) Ground state phase diagram for the bound (BP) to unbound (UP) transition of the two-atom polaritons in g_0-$(a_s)^{-1}$ plane. The photon number $n_{\rm ph}$ and the singlet population in the ground state for $\delta = 0$ and $(k_c a_s)^{-1} = 1$ as functions of $\sqrt{N}g_0/E_c$ are plotted in (c) and (d), respectively. Both of these quantities exhibit discontinous jump across the transition point. Differet lines correspond to different excitation numbers N as indicated in the figure. The photon number $n_{\rm ph}$ plotted in (c) is downshifted by $N-1$.

The ground state BP possesses COM momentum $\mathbf{q}_{\rm BP} = q_{\rm BP}\hat{\mathbf{e}}_z$ which minimizes $E_{\mathbf{q}}$. In Fig. 2(a) we plot the ground state energy $E_{\rm BP} = E_{\mathbf{q}=\mathbf{q}_{\rm BP}}$ as a function of ALC coupling strength g_0.

The COM momentum $q_{\rm BP}$ and the atom-photon entanglement entropy $S_{\rm BP}$ are plotted in Fig. 2(b) and (c), respectively. It is noteworthy that the COM momentum of the ground state BP is finite when $\delta = 0$. By contrast, under the same resonant condition, when the SOC is induced by classical laser beams, the two-atom bound state always possesses zero COM momentum in the ground state [55].

Note that the curves presented in Fig. 2 all terminate at finite g_0. Beyond this ALC coupling strength, the BP becomes unstable as its energy exceeds the continuum threshold $E_{\rm th}$, which is also the ground state energy of the UP (see discussion earlier). Next, we turn to the transition between the BP and the UP as g_0 is tuned.

Bound to unbound polariton transition. – A BP is only energetically stable, and hence truly bound, when its energy is below the continuum threshould. Therefore, it is instructive to calculate the quantity $\epsilon_b \equiv E_{\mathbf{q}_{\rm BP}} - E_{\rm th}$, which is plotted in Fig. 3(a) as a function of g_0 for a given scattering length $(k_c a_s)^{-1} = 1$. The BP is stable if $\epsilon_b < 0$. As one can see from the figure, stable BP exists for small g_0. As g_0 increases, ϵ_b increases and eventually reaches zero, and the BP is no longer stable. From this calculation, we can thus generate a phase diagram, in the parameter space spanned by g_0 and the inverse scattering length a_s^{-1}, as shown in Fig. 3(b). BP is stable under the curve. Above the curve, BP is unstable and UP represents the true ground state of the system.

The transition between the BP and the UP across the critical ALC coupling strength is of first order. This can be clearly see from the discontinuous jump exhibited by the ground state photon number $n_{\rm ph}$ and the spin singlet population $|\phi_s|^2 = \sum'_{\mathbf{k}} |\varphi_s^{\mathbf{k},\mathbf{q}}|^2$ (see the SM for details) plotted in Fig. 3(c) and (d), respectively. As g_0 increases across the critical point, the ground state changes from BP to the UP, and the photon population jumps upward. On the other hand, the BP is dominated by the singlet component due to the strong s-wave interaction, and the singlet population suddenly vanishes across the critical point as the UP is purely triplet. In addition to the photon and the singlet population, the entanglement entropy also has a sudden jump across the transition point, which can be inferred from Fig. 1(c) and Fig. 2(c).

In the case where the SOC is induced by classical Raman laser beams and in the presence of strong attractive s-interaction, we can also find a bound two-atom dimer state which becomes unbound when the Raman coupling strength exceeds a critical value. This bound to unbound transition is, however, continuous [55]. The first-order transition in our current study is due to the quantum nature of the cavity field. The s-wave interaction favors singlet pairing associated with a relatively small photon population, whereas, as can be seen from the wave function (2), the largest photon component is always associated with a spin triplet state with both atoms occupying the $|\downarrow\rangle$ state. Since a large photon number enhances effective atom-photon coupling and decreases the total energy, there exists a competition between the s-wave interaction and the ALC, which results in the first-order transition observed here.

Discussions. – We first discuss some experimental related issues. Recently, there has been able to create a small but definite number of fermions [56] and homogeneous box potentials both for boson [57] and fermion [58]. Noticing that there has been routinely to couple a Bose-Einstein condensate with a high-finesse optical cavity [1, 2, 5] and a tunable JC-type coupling between atomic internal states and an optical cavity has also been realized [59], and considering that it seems no fundamental difficulty to couple a Fermi gas with an optical cavity, it is possible to realize the model studied in this paper for two atoms in the near future. Near recently, two neutral atoms coupled to a cavity field collectively has been reported [60]. Beyond two atoms, the situations become much more complicated, and besides the bounded two-atom state, other exotic states may exist in the absence of ALC, e.g. the Efimov-type trimer state [61], the polaron [62] and so on. One may expect these states would be also changed dramatically by the ALC. Nevertheless,

the detailed analysis of such states is beyond the scope of this work, and we leave it for the future study.

So far, we focus on the equilibrium behaviors and have neglected the impacts of dissipations. For a realistic atom-cavity system, the most important decay channel is the leakage of cavity photons with decay rate κ. In the good cavity limit, where κ is much smaller than g_0 and U, the system can be viewed in a quasiequilibrium state within timescale $1/\kappa$ and above results can be applied. Recently, the polariton-type spectrum has been observed for a BEC in an optical cavity [1]. While in the bad cavity limit, κ is comparable with (or larger than) other energy scales. To maintain a long-run cavity field, one needs to implement a driven laser field, which does not conserve the polariton number N_p. In that case, the cavity field relaxes to a stationary coherent state in a time scale that is typically faster than the dynamics of the atoms [63]. An appropriate treatment is to replace the photon operators in Eq. (2) with a coherent field, which may lead to a steady-state solution [5].

In conclusion, we have shown that a system of two spin-1/2 fermions coupled to a single-mode cavity field displays a rich variety of physics, due to the interplay between the inter-atomic interaction and the atom-cavity coupling. The atoms and the cavity field form a two-atom polariton. As the atom-cavity coupling strength is tuned, a first-order transition between a bound and an unbound polariton state is observed. Accompanying with this transition, the photon population, atomic spin singlet fraction, atom-photon entanglement entropy, and the momentum of the polariton all exhibit discontinuous jumps. These jumps render the transition readily detectable in experiments. Our work paves a way for future studies of quantum few-body and many-body physics in atom-cavity systems.

This work is supported by NSFC under Grant Nos. 11404225, 11474205, 11504037 and 11434015. Q. Sun, A. C. Ji and L. Wen also acknowledge the support by Foundation of Beijing/Chongqing Education Committees under Grant Nos. CIT&TCD201804074, KM201510028005, KZ201810028043, and KJ1500311. H. P. acknowledges support from the US NSF and the Welch Foundation (Grant No. 1669).

Appendix A: Unbound Two-atom Polariton Continuum

First consider two non-interacting atoms with momenta $\mathbf{k}_{1,2} = \frac{\mathbf{q}}{2} \pm \mathbf{k}$ ($\mathbf{k}, \mathbf{q}$ are the relative and the COM momenta, respectively), the polariton wave function Φ for a given excitation number N can be written as

$$\Phi_{\mathbf{k},\mathbf{q}} = \varphi^{\uparrow\downarrow}_{\mathbf{k},\mathbf{q}}\hat{\psi}^\dagger_{\mathbf{k}_1\uparrow}\hat{\psi}^\dagger_{\mathbf{k}_2\downarrow}|N-1\rangle + \varphi^{\downarrow\uparrow}_{\mathbf{k},\mathbf{q}}\hat{\psi}^\dagger_{\mathbf{k}_1\downarrow}\hat{\psi}^\dagger_{\mathbf{k}_2\uparrow}|N-1\rangle + \varphi^{\uparrow\uparrow}_{\mathbf{k},\mathbf{q}}\hat{\psi}^\dagger_{\mathbf{k}_1\uparrow}\hat{\psi}^\dagger_{\mathbf{k}_2\uparrow}|N-2\rangle + \varphi^{\downarrow\downarrow}_{\mathbf{k},\mathbf{q}}\hat{\psi}^\dagger_{\mathbf{k}_1\downarrow}\hat{\psi}^\dagger_{\mathbf{k}_2\downarrow}|N\rangle, \tag{A1}$$

where $|n\rangle = \frac{1}{\sqrt{n!}}(\hat{a}^\dagger)^n|0\rangle$ denotes the n-photon Fock state. In this case, the Schrödinger equation $\hat{H}_0|\Phi_{\mathbf{k},\mathbf{q}}\rangle = E_{\mathbf{k},\mathbf{q}}|\Phi_{\mathbf{k},\mathbf{q}}\rangle$ can be cast into a matrix form $(\hat{M} - E_{\mathbf{k},\mathbf{q}}\hat{I})\Phi = 0$ with

$$\hat{M} = \begin{pmatrix} \varepsilon_{\mathbf{k}_1,\uparrow} + \varepsilon_{\mathbf{k}_2,\uparrow} + \delta & g_0\sqrt{N-1} & g_0\sqrt{N-1} & 0 \\ g_0\sqrt{N-1} & \varepsilon_{\mathbf{k}_1,\uparrow} + \varepsilon_{\mathbf{k}_2,\downarrow} & 0 & g_0\sqrt{N} \\ g_0\sqrt{N-1} & 0 & \varepsilon_{\mathbf{k}_2,\uparrow} + \varepsilon_{\mathbf{k}_1,\downarrow} & g_0\sqrt{N} \\ 0 & g_0\sqrt{N} & g_0\sqrt{N} & \varepsilon_{\mathbf{k}_1,\downarrow} + \varepsilon_{\mathbf{k}_2,\downarrow} - \delta \end{pmatrix}. \tag{A2}$$

Then, the eigenvalue $E_{\mathbf{k},\mathbf{q}}$ of $\hat{M}$ satisfies

$$\mathcal{E}_{\mathbf{k},\mathbf{q}} = \frac{2(N-1)g_0^2}{\mathcal{E}_{\mathbf{k},\mathbf{q}} - \delta - k_c q_z/2m} + \frac{2Ng_0^2}{\mathcal{E}_{\mathbf{k},\mathbf{q}} + \delta + k_c q_z/2m} + \frac{(k_c k_z)^2}{\mathcal{E}_{\mathbf{k},\mathbf{q}}}, \tag{A3}$$

where $\mathcal{E}_{\mathbf{k},\mathbf{q}} = E_{\mathbf{k},\mathbf{q}} - \epsilon_{\frac{\mathbf{q}}{2}+\mathbf{k}} - \epsilon_{\frac{\mathbf{q}}{2}-\mathbf{k}} - \frac{k_c^2}{4m} - (N-1)\hbar\omega_c$ with $\epsilon_{\mathbf{k}} = \frac{\mathbf{k}^2}{2m}$. As indicated in the context, the lowest

$E_{\mathbf{k},\mathbf{q}}$ defines the threshold value $E_{\rm th}$ of the unbound polariton continuum. Correspondingly, the wavefuntion of each $E_{\mathbf{k},\mathbf{q}}$ is given by

$$\begin{aligned}\varphi_a^{\mathbf{k},\mathbf{q}} &= \frac{1}{\sqrt{\mathcal{C}}}\\ \varphi_s^{\mathbf{k},\mathbf{q}} &= \frac{k_c k_z/m}{\mathcal{E}_{\mathbf{k},\mathbf{q}}}\varphi_a^{\mathbf{k},\mathbf{q}}\\ \varphi_{\mathbf{k},\mathbf{q}}^{\uparrow\uparrow} &= \frac{\sqrt{2}g_0\sqrt{N-1}}{\mathcal{E}_{\mathbf{k},\mathbf{q}}-\delta-\frac{k_c q_z}{2m}}\varphi_a^{\mathbf{k},\mathbf{q}}\\ \varphi_{\mathbf{k},\mathbf{q}}^{\downarrow\downarrow} &= \frac{\sqrt{2}g_0\sqrt{N}}{\mathcal{E}_{\mathbf{k},\mathbf{q}}+\delta+\frac{k_c q_z}{2m}}\varphi_a^{\mathbf{k},\mathbf{q}},\end{aligned}$$

where $\varphi_s^{\mathbf{k},\mathbf{q}} = \frac{1}{\sqrt{2}}(\varphi_{\mathbf{k},\mathbf{q}}^{\uparrow\downarrow} - \varphi_{\mathbf{k},\mathbf{q}}^{\downarrow\uparrow})$ and $\varphi_a^{\mathbf{k},\mathbf{q}} = \frac{1}{\sqrt{2}}(\varphi_{\mathbf{k},\mathbf{q}}^{\uparrow\downarrow} + \varphi_{\mathbf{k},\mathbf{q}}^{\downarrow\uparrow})$, and $\mathcal{C}$ is the normalization constant such that

$$|\varphi_s^{\mathbf{k},\mathbf{q}}|^2 + |\varphi_a^{\mathbf{k},\mathbf{q}}|^2 + |\varphi_{\mathbf{k},\mathbf{q}}^{\uparrow\uparrow}|^2 + |\varphi_{\mathbf{k},\mathbf{q}}^{\downarrow\downarrow}|^2 = 1.$$

The corresponding photon population is given by

$$n_{\rm ph} \equiv \langle \hat{a}^\dagger \hat{a}\rangle = (N-1) + |\varphi_{\mathbf{k},\mathbf{q}}^{\downarrow\downarrow}|^2 - |\varphi_{\mathbf{k},\mathbf{q}}^{\uparrow\uparrow}|^2 .$$

For the ground state, one can always find $k_z = 0$. Then, we have $\varphi_s^{\mathbf{k},\mathbf{q}} = 0$ and, as a result, the singlet component in the ground state unbound polariton wave function $\Phi_{\mathbf{k},\mathbf{q}}$ vanishes. Such a state remains an eigenstate of the full Hamiltonian when interaction term $\hat{H}_{\rm int}$ is included. As it can be straightforwardly show that $\hat{H}|\Phi_{\mathbf{k},\mathbf{q}}\rangle_G = (\hat{H}_0 + \hat{H}_{\rm int})|\Phi_{\mathbf{k},\mathbf{q}}\rangle_G = \hat{H}_0|\Phi_{\mathbf{k},\mathbf{q}}\rangle_G = E_{\mathbf{k},\mathbf{q}}|\Phi_{\mathbf{k},\mathbf{q}}\rangle_G$.

To determine the COM momentum $q_{\rm UP}$ of the ground state at $\delta = 0$, we first setting $k_z = 0$ in Eq. A3, which results in a cubic equation of $\mathcal{E}_{0,q_z}$: $\mathcal{E}_{0,q_z}(\mathcal{E}_{0,q_z} - \frac{k_c q_z}{2m})(\mathcal{E}_{0,q_z} + \frac{k_c q_z}{2m}) = (4N-2)g_0^2\mathcal{E}_{0,q_z} - g_0^2\frac{k_c q_z}{m}$. Solving E_{0,q_z} from above $\mathcal{E}_{0,q_z}$, and further minimizing it with respect to q_z, one can obtain $q_{\rm UP}$. There are two limits (discussed in the main text) : (1) For small g_0, $E_{0,q_z}/E_c \simeq \frac{1}{2}(q_z/k_c)^2 - \sqrt{(q_z/k_c)^2 + (4N-2)(g_0/E_c)^2} - 2g_0^2 + o(g_0^2)$, $q_{\rm UP} \simeq k_c\sqrt{1-(4N-2)(g_0/E_c)^2}$; (2) For large g_0, $E_{0,q_z}/E_c \simeq -\sqrt{4N-2}(g_0/E_c) + \frac{1}{2}(q_z/k_c)^2 - \frac{1}{4N-2}(q_z/k_c) + O(g_0^{-1})$, $q_{\rm UP} \simeq \frac{k_c}{4N-2}$.

Appendix B: The Bound Polariton

For given excitation number N, the wave function of a bound polariton (BP) can be generally constructed as

$$\Psi_{\mathbf{q}} = \sum_{\mathbf{k}}{}' \Phi_{\mathbf{k},\mathbf{q}} = \sum_{\mathbf{k}}{}' \Big\{ \varphi_{\mathbf{k},\mathbf{q}}^{\uparrow\downarrow}\hat{\psi}_{\mathbf{k}_1\uparrow}^\dagger\hat{\psi}_{\mathbf{k}_2\downarrow}^\dagger|N-1\rangle + \varphi_{\mathbf{k},\mathbf{q}}^{\downarrow\uparrow}\hat{\psi}_{\mathbf{k}_1\downarrow}^\dagger\hat{\psi}_{\mathbf{k}_2\uparrow}^\dagger|N-1\rangle + \varphi_{\mathbf{k},\mathbf{q}}^{\uparrow\uparrow}\hat{\psi}_{\mathbf{k}_1\uparrow}^\dagger\hat{\psi}_{\mathbf{k}_2\uparrow}^\dagger|N-2\rangle + \varphi_{\mathbf{k},\mathbf{q}}^{\downarrow\downarrow}\hat{\psi}_{\mathbf{k}_1\downarrow}^\dagger\hat{\psi}_{\mathbf{k}_2\downarrow}^\dagger|N\rangle \Big\}, \quad \text{(B1)}$$

where $\mathbf{q}$ is the COM momentum and the summation over the relative momentum $\sum_{\mathbf{k}}'$ is limited to $k_z > 0$. Substituting $\Psi_{\mathbf{q}}$ into the Schrödinger equation $\hat{H}|\Psi_{\mathbf{q}}\rangle = E_{\mathbf{q}}|\Psi_{\mathbf{q}}\rangle$ and writing it explicitly, we obtain

$$\Big\{E_{\mathbf{q}} - (\epsilon_{\frac{\mathbf{q}}{2}+\mathbf{k},\uparrow} + \epsilon_{\frac{\mathbf{q}}{2}-\mathbf{k},\downarrow}) - (N-1)\omega_c\Big\}\varphi_{\mathbf{k},\mathbf{q}}^{\uparrow\downarrow} = \frac{U}{V}\sum_{\mathbf{k}'}{}'(\varphi_{\mathbf{k}',\mathbf{q}}^{\uparrow\downarrow} - \varphi_{\mathbf{k}',\mathbf{q}}^{\downarrow\uparrow}) + g_0\sqrt{N}\varphi_{\mathbf{k},\mathbf{q}}^{\downarrow\downarrow} + g_0\sqrt{N-1}\varphi_{\mathbf{k},\mathbf{q}}^{\uparrow\uparrow} \quad \text{(B2)}$$

$$\Big\{E_{\mathbf{q}} - (\epsilon_{\frac{\mathbf{q}}{2}+\mathbf{k},\downarrow} + \epsilon_{\frac{\mathbf{q}}{2}-\mathbf{k},\uparrow}) - (N-1)\omega_c\Big\}\varphi_{\mathbf{k},\mathbf{q}}^{\downarrow\uparrow} = -\frac{U}{V}\sum_{\mathbf{k}'}{}'(\varphi_{\mathbf{k}',\mathbf{q}}^{\uparrow\downarrow} - \varphi_{\mathbf{k}',\mathbf{q}}^{\downarrow\uparrow}) + g_0\sqrt{N}\varphi_{\mathbf{k},\mathbf{q}}^{\downarrow\downarrow} + g_0\sqrt{N-1}\varphi_{\mathbf{k},\mathbf{q}}^{\uparrow\uparrow} \quad \text{(B3)}$$

$$\Big\{E_{\mathbf{q}} - \delta - (\epsilon_{\frac{\mathbf{q}}{2}+\mathbf{k},\uparrow} + \epsilon_{\frac{\mathbf{q}}{2}-\mathbf{k},\uparrow}) - (N-1)\omega_c\Big\}\varphi_{\mathbf{k},\mathbf{q}}^{\uparrow\uparrow} = g_0\sqrt{N-1}(\varphi_{\mathbf{k},\mathbf{q}}^{\uparrow\downarrow} + \varphi_{\mathbf{k},\mathbf{q}}^{\downarrow\uparrow}) \quad \text{(B4)}$$

$$\Big\{E_{\mathbf{q}} + \delta - (\epsilon_{\frac{\mathbf{q}}{2}+\mathbf{k},\downarrow} + \epsilon_{\frac{\mathbf{q}}{2}-\mathbf{k},\downarrow}) - (N-1)\omega_c\Big\}\varphi_{\mathbf{k},\mathbf{q}}^{\downarrow\downarrow} = g_0\sqrt{N}(\varphi_{\mathbf{k},\mathbf{q}}^{\uparrow\downarrow} + \varphi_{\mathbf{k},\mathbf{q}}^{\downarrow\uparrow}). \quad \text{(B5)}$$

Introducing $\mathcal{E}'_{\mathbf{k},\mathbf{q}} = E_{\mathbf{q}} - \epsilon_{\frac{\mathbf{q}}{2}+\mathbf{k}} - \epsilon_{\frac{\mathbf{q}}{2}-\mathbf{k}} - \frac{k_c^2}{4} - (N-1)\hbar\omega_c$, and defining $\varphi_s^{\mathbf{k},\mathbf{q}} = \frac{1}{\sqrt{2}}(\varphi_{\mathbf{k},\mathbf{q}}^{\uparrow\downarrow} - \varphi_{\mathbf{k},\mathbf{q}}^{\downarrow\uparrow})$ and $\varphi_a^{\mathbf{k},\mathbf{q}} = \frac{1}{\sqrt{2}}(\varphi_{\mathbf{k},\mathbf{q}}^{\uparrow\downarrow} + \varphi_{\mathbf{k},\mathbf{q}}^{\downarrow\uparrow})$, Eqs. (9-12) turn to

$$\mathcal{E}'_{\mathbf{k},\mathbf{q}}\varphi_a^{\mathbf{k},\mathbf{q}} - \frac{k_c k_z}{m}\varphi_s^{\mathbf{k},\mathbf{q}} = \sqrt{2}g_0\sqrt{N}\varphi_{\mathbf{k},\mathbf{q}}^{\downarrow\downarrow} + \sqrt{2}g_0\sqrt{N-1}\varphi_{\mathbf{k},\mathbf{q}}^{\uparrow\uparrow} \tag{B6}$$

$$\mathcal{E}'_{\mathbf{k},\mathbf{q}}\varphi_s^{\mathbf{k},\mathbf{q}} - \frac{k_c k_z}{m}\varphi_a^{\mathbf{k},\mathbf{q}} = \frac{2U}{V}\sum_{\mathbf{k}'}{}' \varphi_s^{\mathbf{k}',\mathbf{q}} \tag{B7}$$

$$\{\mathcal{E}'_{\mathbf{k},\mathbf{q}} - \delta - \frac{k_c q_z}{2m}\}\varphi_{\mathbf{k},\mathbf{q}}^{\uparrow\uparrow} = \sqrt{2}g_0\sqrt{N-1}\varphi_a^{\mathbf{k},\mathbf{q}} \tag{B8}$$

$$\{\mathcal{E}'_{\mathbf{k},\mathbf{q}} + \delta + \frac{k_c q_z}{2m}\}\varphi_{\mathbf{k},\mathbf{q}}^{\downarrow\downarrow} = \sqrt{2}g_0\sqrt{N}\varphi_a^{\mathbf{k},\mathbf{q}}. \tag{B9}$$

From above equations, a nontrivial bound state solution $E_{\mathbf{q}}$ (derived from the coefficient of singlet φ_s) can be found, which satisfies the following self-consistent equation (as in the context)

$$\frac{m}{4\pi\hbar^2 a_s} = \frac{1}{V}\sum_{\mathbf{k}}[(\mathcal{E}'_{\mathbf{k},\mathbf{q}} - \frac{k_c^2 k_z^2/m^2}{\mathcal{E}'_{\mathbf{k},\mathbf{q}} - \frac{2Ng_0^2}{\mathcal{E}'_{\mathbf{k},\mathbf{q}}+\delta+k_c q_z/2m} - \frac{2(N-1)g_0^2}{\mathcal{E}'_{\mathbf{k},\mathbf{q}}-\delta-k_c q_z/2m}})^{-1} + \frac{1}{2\epsilon_{\mathbf{k}}}]. \tag{B10}$$

The ground BP state is determined by further minimizing $E_{\mathbf{q}}$ with respect to the COM momentum $\mathbf{q}$.

Once the energy $E_{\mathbf{q}}$ is solved from Eq. (B10), one can obtain the wave function $\Psi_{\mathbf{q}}$ straightforwardly, with the coefficients giving by

$$\varphi_s^{\mathbf{k},\mathbf{q}} = \frac{1}{\sqrt{\mathcal{C}'}}(\mathcal{E}'_{\mathbf{k},\mathbf{q}} - \frac{k_c^2 k_z^2/m^2}{\mathcal{E}'_{\mathbf{k},\mathbf{q}} - \frac{2Ng_0^2}{\mathcal{E}'_{\mathbf{k},\mathbf{q}}+\delta+k_c q_z/2m} - \frac{2(N-1)g_0^2}{\mathcal{E}'_{\mathbf{k},\mathbf{q}}-\delta-k_c q_z/2m}})^{-1} \tag{B11}$$

$$\varphi_a^{\mathbf{k},\mathbf{q}} = \frac{k_c k_z/m}{\mathcal{E}'_{\mathbf{k},\mathbf{q}} - \frac{2Ng_0^2}{\mathcal{E}'_{\mathbf{k},\mathbf{q}}+\delta+k_c q_z/2m} - \frac{2(N-1)g_0^2}{\mathcal{E}'_{\mathbf{k},\mathbf{q}}-\delta-k_c q_z/2m}}\varphi_s^{\mathbf{k},\mathbf{q}} \tag{B12}$$

$$\varphi_{\mathbf{k},\mathbf{q}}^{\uparrow\uparrow} = \frac{\sqrt{2}g_0\sqrt{N-1}}{\mathcal{E}'_{\mathbf{k},\mathbf{q}} - \delta - \frac{k_c q_z}{2m}}\varphi_a^{\mathbf{k},\mathbf{q}} \tag{B13}$$

$$\varphi_{\mathbf{k},\mathbf{q}}^{\downarrow\downarrow} = \frac{\sqrt{2}g_0\sqrt{N}}{\mathcal{E}'_{\mathbf{k},\mathbf{q}} + \delta + \frac{k_c q_z}{2m}}\varphi_a^{\mathbf{k},\mathbf{q}}, \tag{B14}$$

where constant $\mathcal{C}'$ is the normalization constant such that $\sum'_{\mathbf{k}}\{|\varphi_s^{\mathbf{k},\mathbf{q}}|^2 + |\varphi_a^{\mathbf{k},\mathbf{q}}|^2 + |\varphi_{\mathbf{k},\mathbf{q}}^{\uparrow\uparrow}|^2 + |\varphi_{\mathbf{k},\mathbf{q}}^{\downarrow\downarrow}|^2\} = 1$. Apparently, the coefficients of the above triplet components are asymmetric and depend on the excitation number N and the COM momentum q_z. The photon population in the BP state is then given by $n_{\rm ph} = (N-1) + \sum'_{\mathbf{k}}(|\varphi_{\mathbf{k},\mathbf{q}}^{\downarrow\downarrow}|^2 - |\varphi_{\mathbf{k},\mathbf{q}}^{\uparrow\uparrow}|^2)$. And the spin singlet population plotted in Fig. 3(d) in the main text is defined as $|\phi_s|^2 = \sum'_{\mathbf{k}}|\varphi_s^{\mathbf{k},\mathbf{q}}|^2$.

Appendix C: Entanglement Entropy

The von Neumann entanglement entropy for a bipartite system H_{AB} $(= H_A \otimes H_B)$ is defined as

$$S_A \equiv -\mathrm{tr}\rho_A \ln \rho_A. \tag{C1}$$

Here, $\rho_A = \mathrm{tr}_B\rho$ is the reduced density matrix of subsystem A by tracing all degrees of freedom in subsystem B. Notice that, for a pure state, $S_A = S_B$. In our case, the total system is comprised of the atom and photon part, and exhibits nontrivial entanglement properties between

them. For the Bound Polariton, $\rho_{\rm BP} = |\Phi_{\mathbf{q}}\rangle\langle\Phi_{\mathbf{q}}|$, and

$$S_{\rm BP} = -\left\{ \sum_{\mathbf{k}}{}' (|\varphi_s^{\mathbf{k},\mathbf{q}}|^2 + |\varphi_a^{\mathbf{k},\mathbf{q}}|^2) \ln \sum_{\mathbf{k}}{}' (|\varphi_s^{\mathbf{k},\mathbf{q}}|^2 + |\varphi_a^{\mathbf{k},\mathbf{q}}|^2) + \sum_{\mathbf{k}}{}' |\varphi_{\mathbf{k},\mathbf{q}}^{\uparrow\uparrow}|^2 \ln \sum_{\mathbf{k}}{}' |\varphi_{\mathbf{k},\mathbf{q}}^{\uparrow\uparrow}|^2 + \sum_{\mathbf{k}}{}' |\varphi_{\mathbf{k},\mathbf{q}}^{\downarrow\downarrow}|^2 \ln \sum_{\mathbf{k}}{}' |\varphi_{\mathbf{k},\mathbf{q}}^{\downarrow\downarrow}|^2 \right\}. \quad \text{(C2)}$$

For the Unbound Polariton Continuum, $\rho_{\rm UP} = |\Phi_{\mathbf{k},\mathbf{q}}\rangle\langle\Phi_{\mathbf{k},\mathbf{q}}|$, and

$$S_{\rm UP} = -\left\{ (|\varphi_s^{\mathbf{k},\mathbf{q}}|^2 + |\varphi_a^{\mathbf{k},\mathbf{q}}|^2) \ln(|\varphi_s^{\mathbf{k},\mathbf{q}}|^2 + |\varphi_a^{\mathbf{k},\mathbf{q}}|^2) + |\varphi_{\mathbf{k},\mathbf{q}}^{\uparrow\uparrow}|^2 \ln |\varphi_{\mathbf{k},\mathbf{q}}^{\uparrow\uparrow}|^2 + |\varphi_{\mathbf{k},\mathbf{q}}^{\downarrow\downarrow}|^2 \ln |\varphi_{\mathbf{k},\mathbf{q}}^{\downarrow\downarrow}|^2 \right\}. \quad \text{(C3)}$$

[1] F. Brennecke, T. Donner, S. Ritter, T. Bourdel, M. Köhl, and T. Esslinger, Nature **450**, 268 (2007).
[2] Y. Colombe, T. Steinmetz, G. Dubois, F. Linke, D. Hunger, and J. Reichel, Nature **450**, 272 (2007).
[3] J. Larson, B. Damski, G. Morigi, and M. Lewenstein, Phys. Rev. Lett. **100**, 050401 (2008); J. Larson, S. Femández-Vidal, G. Morigi, and M. Lewenstein, New J. Phys. **10**, 045002 (2008).
[4] I. B Mekhov and H. Ritsch, J. Phys. B: At. Mol. Opt. Phys. **45**, 102001 (2012).
[5] H. Ritsch, P. Domokos, F. Brennecke, and T. Esslinger, Rev. Mod. Phys. **85**, 553 (2013).
[6] F. Dimer, B. Estienne, A. S. Parkins, and H. J. Carmichael, Phys. Rev. A **75**, 013804 (2007).
[7] S. Gopalakrishnan, B. L. Lev, and P. M. Goldbart, Nat. Phys. **5**, 845 (2009); *ibid*, Phys. Rev. A **82**, 043612 (2010); *ibid*, Phys. Rev. Lett. **107**, 277201 (2011).
[8] P. Strack and S. Sachdev, Phys. Rev. Lett. **107**, 277202 (2011); M. Müller, P. Strack, and S. Sachdev, Phys. Rev. A **86**, 023604 (2012).
[9] K. Baumann, C. Guerlin, F. Brennecke, and T. Esslinger, Nature **464**, 1301 (2010); K. Baumann, R. Mottl, F. Brennecke, and T. Esslinger, Phys. Rev. Lett. **107**, 140402 (2011).
[10] H. Keßler, J. Klinder, M. Wolke, and A. Hemmerich, Phys. Rev. Lett. **113**, 070404 (2014).
[11] M. P. Baden, K. J. Arnold, A. L. Grimsmo, S. Parkins, and M. D. Barrett, Phys. Rev. Lett. **113**, 020408 (2014).
[12] J. Keeling, M. J. Bhaseen, and B. D. Simons, Phys. Rev. Lett. **112**, 143002 (2014).
[13] F. Piazza and P. Strack, Phys. Rev. Lett. **112** 143003 (2014).
[14] Y. Chen, Z. Yu, and H. Zhai, Phys. Rev. Lett. **112**, 143004 (2014).
[15] H. Habibian, A. Winter, S. Paganelli, H. Rieger, and G. Morigi, Phys. Rev. Lett. **110**, 075304 (2013).
[16] X. F. Zhang, Q. Sun, Y. C. Wen, W. M. Liu, S. Eggert, and A. C. Ji, Phys. Rev. Lett. **110**, 090402 (2013).
[17] F. Piazza and H. Ritsch, Phys. Rev. Lett. **115**, 163601 (2015).
[18] Axel U. J. Lode and C. Bruder, Phys. Rev. Lett. **118**, 013603 (2017).
[19] J. Klinder, H. Keßler, M. R. Bakhtiari, M. Thorwart, and A. Hemmerich, Phys. Rev. Lett. **115**, 230403 (2015).
[20] R. Landig, L. Hruby, N. Dogra, M. Landini, R. Mottl, T. Donner, and T. Esslinger, Nature **532**, 476 (2016).
[21] M. R. Bakhtiari, A. Hemmerich, H. Ritsch, and M. Thorwart, Phys. Rev. Lett. **114**, 123601 (2015).
[22] S. F. Caballero-Benitez and I. B. Mekhov, Phys. Rev. Lett. **115**, 243604 (2015).
[23] J. Leonard, A. Morales, P. Zupancic, T. Esslinger, and T. Donner, Nature **543**, 87 (2017).
[24] C. Kollath, A. Sheikhan, S. Wolff, and F. Brennecke, Phys. Rev. Lett. **116**, 060401 (2016).
[25] A. Sheikhan, F. Brennecke, and C. Kollath, Phys. Rev. A **93** 043609 (2016); A. Sheikhan, F. Brennecke, and C. Kollath, Phys. Rev. A **94**, 061603(R) (2016).
[26] W. Zheng and N. R. Cooper, Phys. Rev. Lett. **117**, 175302 (2016).
[27] K. E. Ballantine, B. L. Lev, and J. Keeling, Phys. Rev. Lett. **118**, 045302 (2017).
[28] F. Mivehvar, H. Ritsch, and F. Piazza, Phys. Rev. Lett. **118**, 073602 (2017); F. Mivehvar, F. Piazza, and H. Ritsch, Phys. Rev. Lett. **119**, 063602 (2017).
[29] Y. K. Wang and F. T. Hioe, Phys. Rev. A **7**, 831 (1973).
[30] K. Hepp and E. H. Lieb, Phys. Rev. A **8**, 2517 (1973); K. Hepp and E. H. Lieb, Ann. Phys. **76**, 360 (1973).
[31] Y.-J. Lin, K. Jiménez-García, and I. B. Spielman, Nature (London) **471**, 83 (2011).
[32] J.-Y. Zhang, S.-C. Ji, Z. Chen, L. Zhang, Z.-D. Du, B. Yan, G.-S. Pan, B. Zhao, Y.-J. Deng, H. Zhai, S. Chen, and J.-W. Pan, Phys. Rev. Lett. **109**, 115301 (2012).
[33] P. J. Wang, Z.-Q. Yu, Z. K. Fu, J. Miao, L. H. Huang, S. J. Chai, H. Zhai, and J. Zhang, Phys. Rev. Lett. **109**, 095301 (2012).
[34] L. W. Cheuk, A. T. Sommer, Z. Hadzibabic, T. Yefsah,

W. S. Bakr, and M. W. Zwierlein, Phys. Rev. Lett. **109**, 095302 (2012).
[35] C. Qu, C. Hamner, M. Gong, C. W. Zhang, P. Engels, Phys. Rev. A **88**, 021604(R) (2013).
[36] J. Li, W. Huang, B. Shteynas, S. Burchesky, F. C. Top, E. Su, J. Lee, A. O. Jamison, and W. Ketterle, Phys. Rev. Lett. **117**, 185301 (2016).
[37] J. Dalibard, F. Gerbier, G. Juzeliūnas, and P. Öhberg, Rev. Mod. Phys. **83**, 1523 (2011).
[38] H. Zhai, Int. J. Mod. Phys. B **26**, 1230001 (2013).
[39] V. Galitski and I. B. Spielman, Nature **494**, 49 (2013).
[40] N. Goldman, G. Juzeliūnas, P. Öhberg, and I. B. Spielman, Rep. Prog. Phys. **77**, 126401 (2014).
[41] X. F. Zhou, Y. Li, Z. Cai, and C. J. Wu, J. Phys. B: At. Mol. Opt. Phys. **46**, 134001 (2013).
[42] H. Zhai, Rep. Prog. Phys. **78**, 026001 (2015).
[43] Y. Deng, J. Cheng, H. Jing, and S. Yi, Phys. Rev. Lett. **112**, 143007 (2014).
[44] L. Dong, L. Zhou, B. Wu, B. Ramachandhran, and H. Pu, Phys. Rev. A **89**, 011602(R) (2014); L. Dong, C. Zhu, and H. Pu, Atoms **3**, 182 (2015).
[45] F. Mivehvar and D. L. Feder, Phys. Rev. A **89**, 013803 (2014).
[46] B. Padhi and S. Ghosh, Phys. Rev. A **90**, 023627 (2014).
[47] J.-S. Pan, X. J. Liu, W. Zhang, W. Yi, and G. C. Guo, Phys. Rev. Lett. **115**, 045303 (2015).
[48] D. Kruse, C. von Cube, C. Zimmermann, and P. W. Courteille, Phys. Rev. Lett. **91**, 183601 (2003).
[49] J. Klinner, M. Lindholdt, B. Nagorny, and A. Hemmerich, Phys. Rev. Lett. **96**, 023002 (2006).
[50] S. Slama, G. Krenz, S. Bux, C. Zimmermann, and P. W. Courteille, Phys. Rev. A **75**, 063620 (2007).
[51] When the internal excited state is far-detuned from the cavity field, the adiabatic elimination of the excited state could give rise to a state-independent but position-dependent phase factor, which can not be eliminated as in [50].
[52] S. Giorgini, L. P. Pitaevskii, S. Stringari, Rev. Mod. Phys. **80**, 1215 (2008).
[53] C. Zhu, L. Dong, and H. Pu, Phys. Rev. A **94**, 053621 (2016).
[54] On the BEC side of the BEC-BCS crossover, there is a shallow bound state for an attractive inter-atomic contact interaction with positive scattering length $a_s > 0$, meaning that the scattering wave is "repulsive" even though the underlying potential is attractive.
[55] L. Dong, L. Jiang, H. Hu, and H. Pu, Phys. Rev. A **87**, 043616 (2013).
[56] F. Serwane, G. Zürn, T. Lompe, T. B. Ottenstein, A. N. Wenz, and S. Jochim, Science **332**, 336 (2011).
[57] A. L. Gaunt, T. F. Schmidutz, I. Gotlibovych, R. P. Smith, and Z. Hadzibabic, Phys. Rev. Lett. **110**, 200406 (2013).
[58] B. Mukherjee, Z. Yan, P. B. Patel, Z. Hadzibabic, T. Yefsah, J. Struck, and M. W. Zwierlein, Phys. Rev. Lett. **118**, 123401 (2017).
[59] M. P. Baden, K. J. Arnold, A. L. Grimsmo, S. Parkins, and M. D. Barrett, Phys. Rev. Lett. **113**, 020408 (2014).
[60] R. Reimann, W. Alt, T. Kampschulte, T. Macha, L. Ratschbacher, N. Thau, S. Yoon, and D. Meschede, Phys. Rev. Lett. **114**, 023601 (2015).
[61] P. Naidon and S. Endo, Rep. Prog. Phys. **80**, 056001 (2017).
[62] S. Zöllner, G. M. Bruun, and C. J. Pethick, Phys. Rev. A **83**, 021603 (2011).
[63] D. Nagy, J. K. Asbth, P. Domokos, and H. Ritsch, Europhys. Lett. **74**, 254 (2006).